SHORT-BASELINE ACTIVE TRIANGULATION FOR CAD RECONSTRUCTION OF ROOM-SIZED INDUSTRIAL ENVIRONMENTS

David Chapman[*], Sabry El-Hakim[**]

[*]University College London, UK
Department of Geomatic Engineering
dchapman@ge.ucl.ac.uk
[**]National Research Council of Canada, Canada
Visual Information Technology Group
Sabry.El-Hakim@iit.nrc.ca

Working Group V/3

KEY WORDS: Active Triangulation, Range Imaging, As-Built Surveys

ABSTRACT

Recent developments in non-contact industrial range imaging systems have generally focussed either on very high-precision, short range, active triangulation systems capable of detailing measurement volumes of a few square metres or medium precision, time-of-flight systems with typical standoff distances of 2-50 metres. This paper will highlight a range of applications for medium precision (+/- 5mm) imaging of relatively complex, room-sized environments which are not currently well served by such systems. It will also suggest that the development of relatively short baseline active triangulation systems may lead to affordable, compact and robust short-range measurement systems capable of delivering range data suitable for such applications. A brief review of current systems for non-contact range-imaging will be followed by a detailed discussion of system trials undertaken with a modified Biris triangulation system in a typical engineering environment containing a wide variety industrial surfaces with a range of surface reflectivity characteristics. The authors will conclude that such a system may offer a compact and flexible alternative to competing technologies that could be readily deployed in complex small-scale industrial settings.

1 BACKGROUND

Many authors have documented an increasing demand for as-built modelling of large industrial facilities. Applications of such models range from very accurate surveys of tie-in locations to ensure first-time fit of new components to relatively crude volumetric models suitable for planning access or general facility management operations. One of the difficulties associated with such surveys is the development of appropriate specifications to ensure that measurements are captured at an appropriate density for the anticipated application.

A number of measurement techniques have emerged to serve such markets. These include conventional geodetic surveying techniques based on total station intersection or radiation, close-range photogrammetry and, increasingly, the application of range-imaging sensors.

Theodolite based surveys offer relatively high precision at the expense of comparatively slow data capture times. Since reduction of time spent on site is often of critical importance in such applications these methods are most commonly used for the accurate survey of a few tie-in points required for the fitting of new components and pipe-spools. Photogrammetric surveys can, in certain circumstances, offer comparable measurement precision and have the additional advantage that they enable very rapid data capture and potentially offer complete coverage of the facility for offline measurement. Unfortunately this offline measurement task remains a labour intensive operation that has been stubbornly resistant to attempts to automate image segmentation and object recognition in complex scenes. Against this background range imaging devices appear to have much to offer in that they enable the automatic derivation of dense clouds of 3D on the surfaces of the object. These point clouds offer the potential for some degree of automation of object extraction and thus raise the prospect of cheaper As-Built CAD modelling. Unfortunately many of the early range-imaging systems were often either very expensive, bulky or slow thus offering less flexibility than photogrammetric systems in the very cluttered environments typically encountered in many petrochemical and nuclear environments.

This paper documents an exercise that attempts to assess the utility of a simple, lightweight, robust range-imaging sensor that was felt to be suitable for low-precision survey in the complex and congested environments found typical of offshore oil-platforms.

2 RANGE IMAGING SYSTEMS

Range sensors can generate complete data of visible surfaces that are rather featureless to the human eye or a video camera. Furthermore, they do not require operator-assisted algorithms to generate the 3D coordinates. The disadvantages are that unreliable results may take place on highly reflective surfaces and where sharp range discontinuities exist (El-Hakim and Beraldin, 1994). Furthermore, these 3D active range sensors are usually configured for a specific volume of measurement or range and are not re-configurable. Those designed for large volumes are usually costly and bulky.

2.1 Triangulation-Based Sensors

For applications requiring less than 10-meter range, short and medium range sensors, which are usually based on structured light and triangulation, are often employed. Short range sensors (e.g. ShapeGrabber, http://www.vitana.com) are designed for mainly small objects placed at less than 0.5 m, while medium range (e.g. Cyberware, http://www.cyberware.com) can cover ranges from 0.5 m to 2 m depending on the configuration. They have been used successfully in model creation applied to cultural heritage and space (Beraldin et al, 1998 and 1999). For ranges between 2 m and 10 m, there are a limited number of triangulation-based sensors available. However, some systems have been built with baselines in excess of 1000 mm to cover distances up to 100 m. A sensor with such a baseline has limited usefulness in an application such as ours for lack of compactness. However, a more compact sensor known as the Random Access Camera (RAC) is based on the auto-synchronized scanning (Rioux, 1984) and has a baseline of only 90-mm. It can cover ranges from 0.5m to 10 m. Expected accuracy at the closest range is 0.03 mm but it is about 20 mm at the 10-m range. A short-range sensor will require a much higher number of 3D images; thus the high accuracy of the individual images may be offset by larger error propagation due to registration. Medium range sensors require a lower number of images but the main disadvantage is that the accuracy deteriorates rapidly at longer ranges as expected with triangulation-based sensors.

2.2 Time Of Flight – Time Delay Methods

Long-range sensors, which are capable of covering a large volume of the scene in a single image or perhaps a few images at ranges exceeding 10 meters, are usually based on the time-of-flight (TOF) technology. Data from this type of range sensor scanners, plus texture, has been used for creating VR model of the interior of large structures (Johnson et al, 1997 and Miyatsuka et al, 1998). Although the large volume coverage is very convenient, since the whole scene can be covered with a small number of 3D images, the accuracy is usually in the 10-100 mm range. These scanners also tend to be more costly than shorter-range sensors. For a given site, the choice is now between using a long range sensor that produces less accurate data but with less registration error, or a short to medium-range sensor that produce more accurate data but requires larger number of images resulting in greater registration error. Sensor cost and size are also important factors to consider.

2.3 The ‘Long-Range’ Biris – A Short-Baseline Active Triangulation System

The Biris range imaging system was initially developed by the National Research Council of Canada (NRC) (Blais et al, 1992) and has been adapted for use as a low-cost, highly portable measurement device suited to close-range applications from stand-off distances of the order of 0.3m (Beraldin et.al. 1998).

This experiment sought to evaluate a modified Biris device that had been developed to work over ranges of up to 3m (El-Hakim et al, 1997). The sensor is mounted on a Directed Perception pan/tilt device that enables full panoramic coverage from an image station through the projection and detection of a laser light stripe (figure 1). The pan-tilt unit can be used to scan the 3-D laser profile around a 360° pan angle and a 110° tilt angle. The scanning parameters as well as the image resolution are computer controlled and therefore fully programmable. Different modes of low resolution and high resolution images can be preprogrammed to completely cover the surroundings. A novel iris arrangement in the detector unit coupled with real-time sub-pixel (0.2 pixel) detection of the reflected light stripe supports real-time range determination with a relatively low noise level. The very short baseline employed in the sensor (150mm) enables a robust and compact construction highly suited to this application at the expense of a relatively low precision (table 1).

Figure 1. The Long Range Biris sensor

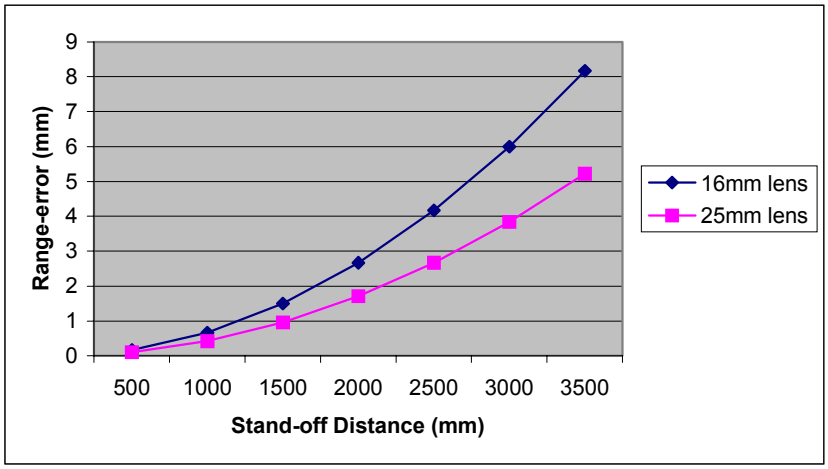

Table 1. Range error for the long range Biris as a function of stand-off distance

Figure 2: The calibration structure.

A calibration structure, covering the views of the Biris scans (partially shown in figure 2), is used to calibrate the 3-D images produced by the Biris and the scanning pan-tilt unit (see El-Hakim et al, 1997, for details). The spherical targets on the structure are surveyed to 0.08 mm accuracy. The estimated accuracy numbers using the targets on the calibration structure as reference are:

RMS(X): 2.27 mm
RMS(Y): 2.44 mm
RMS(Z): 1.87 mm

The results are close to the theoretical expectations computed from sensor resolution and the mathematical model (Table 1). RMS values are obtained from differences between known and computed coordinates.

Thus the system was felt to be capable of delivering range data of sufficient coverage and precision to enable the construction of a crude CAD model suitable for clash determination. This system could be easily integrated within an existing panoramic photogrammetric measurement system that would provide high quality image overlays and the capability to selectively upgrade local measurements. This photogrammetric module would also enable the measurement of small bore piping and cabling that was too small to be resolved in the range-image data.

3 SURVEY OF THE TEST ENVIRONMENT.

Since it was not possible to fully integrate the photogrammetric and range-imaging systems in the budget and timescale of this trial they we deployed separately and brought into a common coordinate framework through the measurement of a number of targeted control points. Figure 3 shows low resolution panoramas generated by the two systems. The partial Biris panorama is generated from four overlapping cylindrical strips each strip comprising 256 x 1024 pixels. A control survey was based upon 11 panoramic photogrammetric stations acquired and localised using the Hazmap remote measurement system (Chapman & Deacon, 1997) with Stereo panoramas being acquired at 4 stations for visualisation purposes. Range images were acquired at 10 locations thus 40 strips of range image data were available for subsequent analysis.

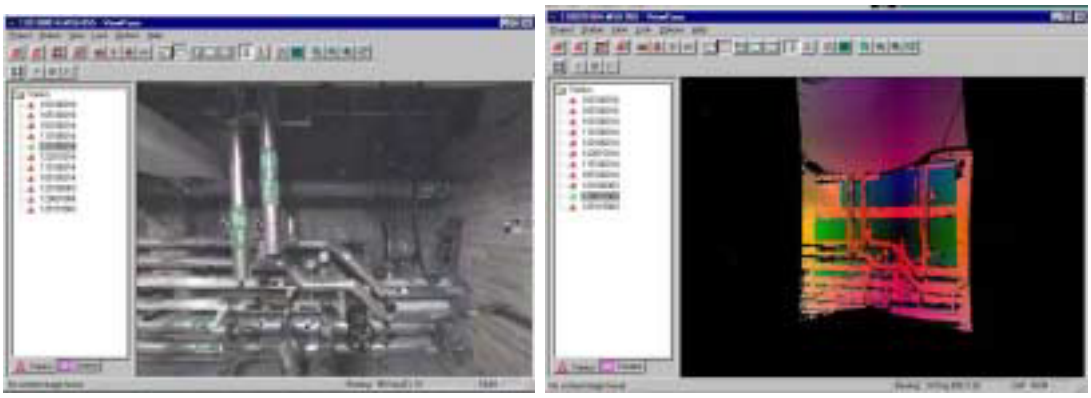

Figure 3. Panoramic image browser with 'Hazmap' image (left) and Biris range image (right).

4 DEVELOPMENT OF TOOLS FOR RANGE IMAGE SEGMENTATION

As can be seem from the images the majority of the features in the scene can be modelled using a limited set of geometric primitives. In order to access the performance of the sensor on the various surfaces in the survey area segmentation tools focussed upon the semi-automatic identification of planar and cylindrical objects. Several techniques were developed and implemented within the MATLAB prototyping environment. These included plane and quadric extraction routines based upon:

- Region growing from user defined seed points;
- Random sampling within user defined region of interest (ROI);
- Random sampling within ROI constrained by step images in the range image.

Of these methods the second proved to be the most efficient enabling robust extraction of the various geometric entities. The method is uses the following algorithm which is based upon that described in more detail by Roth (Roth, 1993)

```
For I = 1 to NumberOfSamples
     Extract a random minimal subset of X,Y,Z coordinates sufficient to determine
     plane or quadric parameters;
     Fit surface to subset;
     Evaluate cost function for current surface based upon all observations;
     If cost is lower than those previously computed mark as best solution;
End;
Reject outlying observations using parameters of best solution;
Evaluate best-fit surface to remaining observations by least-squares estimation;
```

At present the user selects the number of samples taken and the cost function with 1000 random samples generally being sufficient to determine a robust fit. Cost functions in implemented include least-squares measures and the maximum number points falling within user-set error bounds.

4.1 Fitting of quadric surface

The general quadric form is given by equation 1.

$$ax^2 + bxy^2 + cz^2 + 2hxy + 2gxz + 2fyz + ux + vy + wz + 1 = 0 \quad (1)$$

Since we are only interested in planar or cylindrical objects only the linear and quadratic forms were implemented requiring the determination of 3 (u,v,w) and 9 (a..w) parameters respectively. Initial values for a best fitting cylinder are achieved from the analysis of the 9 quadric parameters as described by Fedeema & Little (Feedema & Little, 1997).

4.2 Determination of least-squares cylinder fit.

Cylinder fitting is implemented using the general least squares solution through the iterative refinement of the parameters derived from the quadric fit. The table below shows typical differences between the quadric fit and the final least-squares solution for a number of data sets indicating that the random sampled quadric generally provides good initial values for subsequent least-square analysis (table 2).

	Random sampling of quadric							Least-square fit						
	X_c	Y_c	Z_c	l	m	n	R	X_c	Y_c	Z_c	l	m	n	R
Pipe1	740.90	-2315.08	369.43	0.93	0.36	-0.01	95.39	737.00	-2300.00	366.00	0.93	0.36	-0.01	84.70
	741.00	-2320.00	369.00	0.93	0.36	-0.01	95.40	395.00	-2420.00	364.00	0.92	0.38	-0.04	79.60
	679.00	-2320.00	359.00	0.91	0.43	-0.03	75.00	676.00	-2330.00	365.00	0.94	0.35	0.01	82.70
Pipe2	121.82	-624.10	1210.43	0.34	-0.94	0.01	61.41	119.00	-626.00	1200.00	0.34	-0.94	0.00	52.30
	20.30	-329.00	1220.00	0.33	-0.94	0.03	69.40	14.80	-332.00	1190.00	0.33	-0.94	0.02	50.60
	84.50	-516.00	1210.00	0.34	-0.94	0.01	63.70	80.20	-518.00	1200.00	0.34	-0.94	0.01	52.60
Pipe3	749.00	-2150.00	-476.00	0.92	0.39	-0.03	28.20	751.00	-2160.00	-493.00	0.93	0.38	-0.03	40.70
	507.00	-2240.00	-632.00	-0.64	-0.29	-0.71	26.90	526.00	-2250.00	-644.00	-0.64	-0.29	-0.71	45.40

Table 2. Comparison of initial values from quadric fit using random sampling and least-squares cylinder fit

5 RESULTS OBTAINED

A large number of planar and cylindrical objects were extracted from the range-image data. As anticipated the system exhibited some degradation when attempting to recover data from specular reflectors such as the metal cabinets and aluminium pipe lagging such areas are visible in the intensity image showing areas where the sensor has saturated (figure 4a). The mask image (figure 4c) image also shows the masking of sections of the range image which, although unavoidable in any active triangulation system, are minimised by the short baseline employed in the Biris sensor.

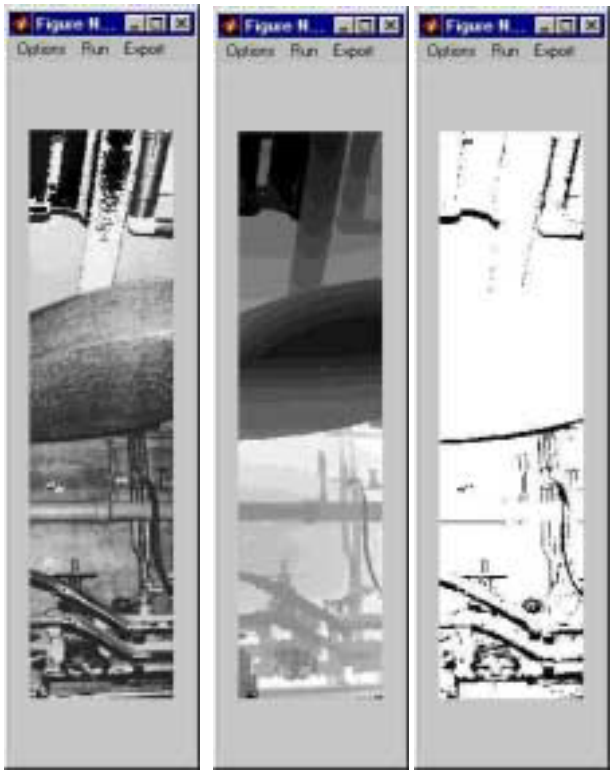

Figure 4 a,b,c. 256 x 1024 Biris intensity, range and mask images (indicating missing or null data). Note dark highlights on piping indicating specular reflections of laser stripe.

Typical RMS errors for cylinder fitting were of the order of 1-2mm and demonstrated good overall agreement with photogrammetric measurements. The measurement strategy involved the identification of major structures which were extracted as planes or cylinders and then removed from the dataset (figures 5 & 6). In this way it was possible to extract the majority of the equipment items and the majority of pipes with radii greater than 40mm. On diffusely reflective surfaces such as the brickwork walls good range data was obtained and it was possible to recover the structure of the surface morphology from a 2-3 metre stand off (figure 8). Small-bore piping could not be reliably extracted and the software did not permit the extraction of more geometries such as circular-torii or complex parts such as valves. These structures were left as isolated clouds of points in the final output. Analysis of the range data as a function of incident angle with respect to the surface normal of a range of reflective surfaces indicate that, as expected, range observations

are degraded at incident angles within 10 degrees of the surface normal. However sufficient data is normally acquired away from these regions to enable a realistic surface recovery. Evidence of such systematic effects can be seen in the pattern of residuals visible in surface fits to both planar (figure 9) and cylindrical data (figure 10).

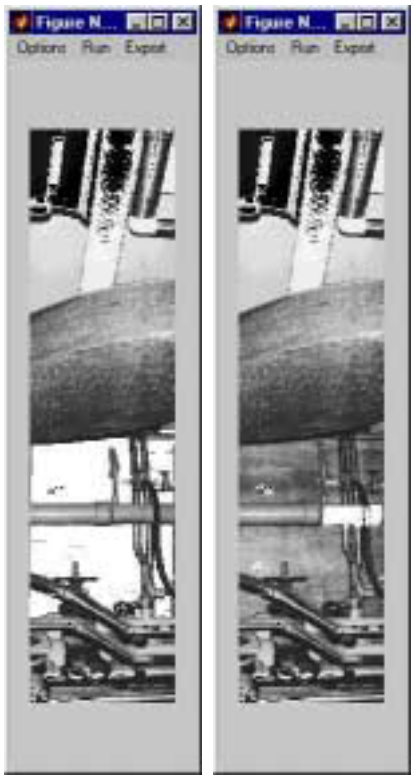

Figure 5. Results of random sampling for user defined region of interest (ROI). The operator first specifies a ROI for a plane fit to the rear wall, points on the wall are identified by the random sampling routine that determines the plane parameters and marks the points as used. Next a ROI for the foreground cylinder is defined.

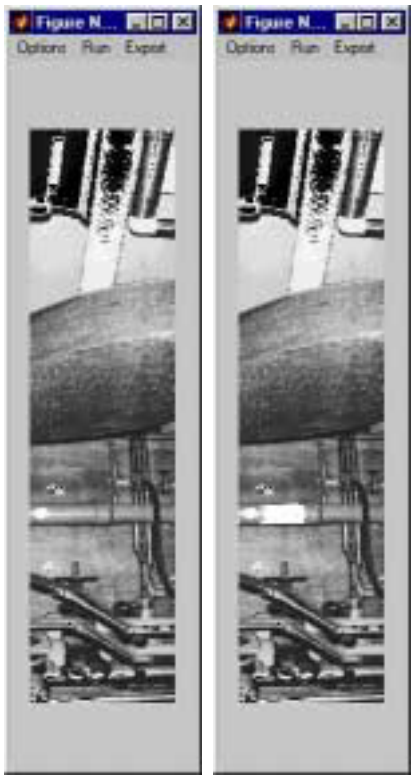

Figure 6. An alternative approach to the extraction of the pipe using an iterative refinement of a best fitting quadric based upon a user-defined seed point (figure 6a) and a pre-defined rejection threshold.

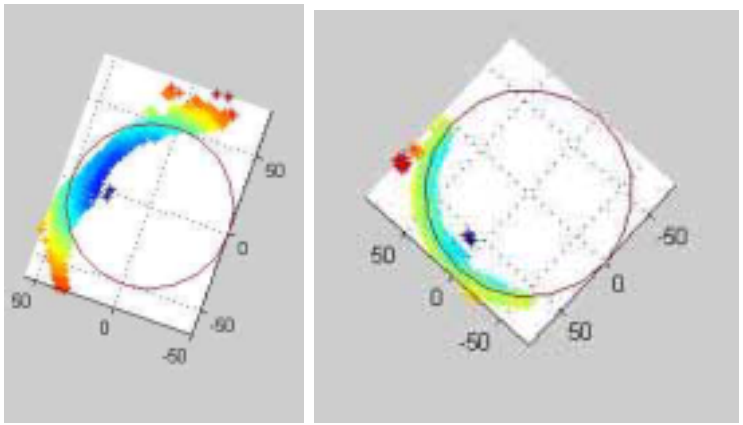

Figure 7. Residuals to initial quadric fit subsequently refined by the least-squares determination of the best fitting cylinder.

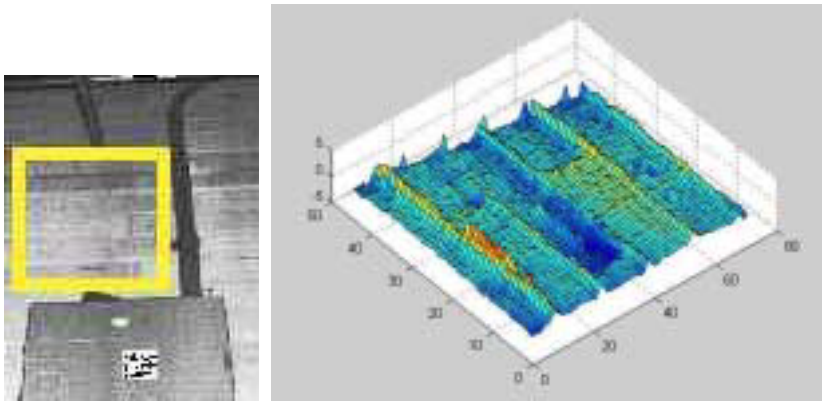

Figure 8. Best fit plane to brick wall with plot of residuals.

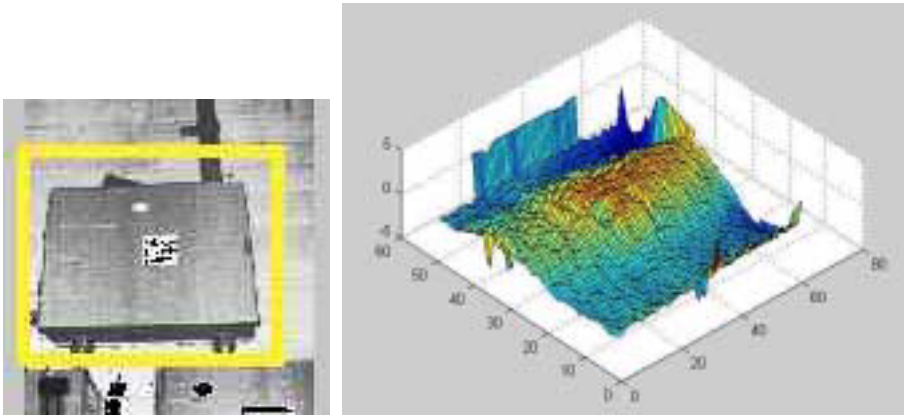

Figure 9. Residuals of plane fit to range image of equipment cabinet.

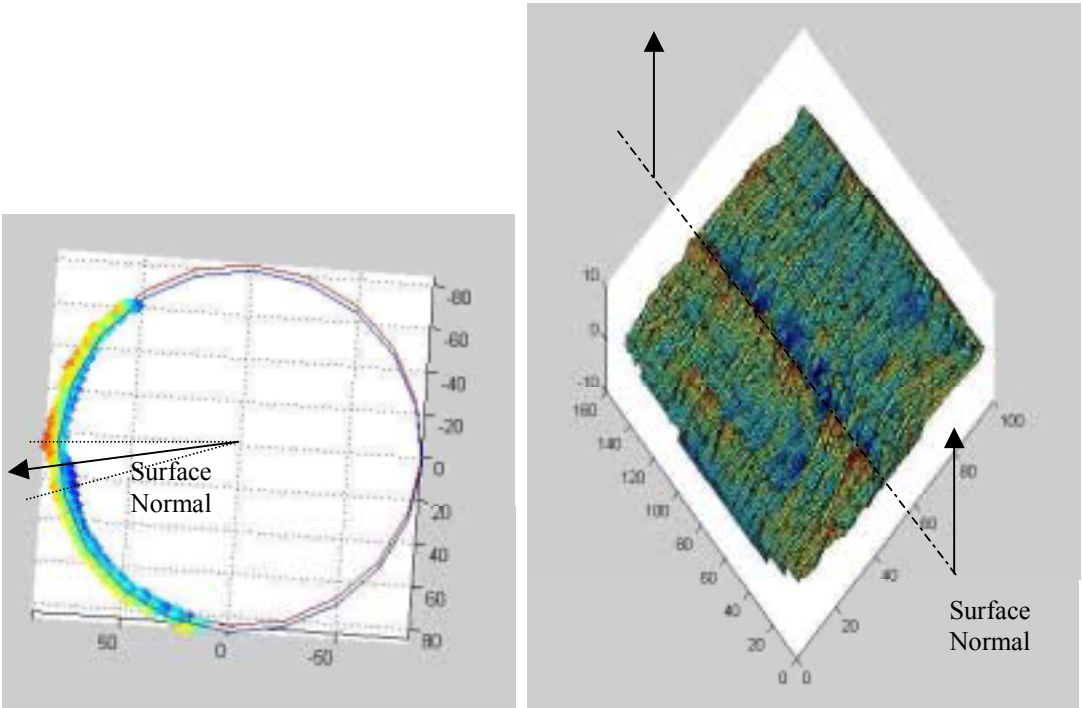

Figure 10. Residuals from cylinder fit to cylinder, RMS = 1.51mm

6 CONCLUSIONS

The Biris system has demonstrated that it is capable of range data recovery from a variety of common surfaces encountered in an industrial setting. Whilst its short baseline configuration means that it will never be capable of millimetric precision over 2-3m stand-off distances it does, never-the-less, enable surface recovery with similar precision to those quoted by the manufacturers of time-of-flight systems. It's compact, robust construction together with lightweight means that such a system would form a very useful additions to the industrial surveyors toolbox.

The recovery of geometric entities from these range images still remains a semi-automatic task. However, the random-sampling strategy describe appears very robust to the noise typically found in such systems when used on a wide variety of surfaces. With the ever-increasing power of desktop computers such 'brute-force' strategies offer considerable potential for further development.

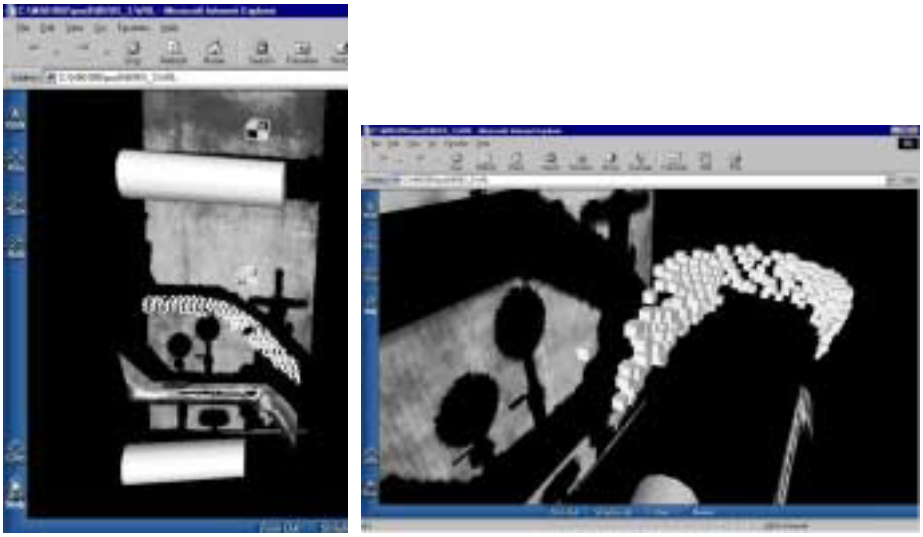

Figure 11. Extracts from a partial VRML model with texture-mapped planar surfaces, cylinders and sub-sampled portions of the original point-cloud.

REFERENCES

Beraldin, J.-A., Blais, F., Cournoyer, L., Rioux, M., Bernier, F., & Harrison, N., 1998. Portable digital 3-d imaging system for remote sites. The 1998 IEEE International Symp. on Circuit and Systems, Monterey, CA, USA: 326-333. May 31-June 3, 1998.

Beraldin, J.A. Blais, F., Cornouyer, L., Rioux, M., El-Hakim, S., 1999. 3D imaging for rapid response on remote sites, SIGGRAPH'99 Technical Sketches, pp. 225, Los Angeles, August 8-13.

Blais, F., LeCavalier, M., Domey, J. Boulanger, P., Courteau, J., 1992. Application of the Biris range sensor for wood-volume measurement. NRC Tech. Report NRC/ERB-1038.

Chapman, D. & Deacon, A., 1997. The role of spatially indexed image archives for "As-Built" modelling of large process plant facilities. Optical 3-D measurement techniques IV, Wichmann, Heidelberg. 300 pages: 475-482.

El-Hakim, S.F., Beraldin, J. -A., 1994. On the integration of range and intensity data to improve vision-based three-dimensional measurements, SPIE Proc., Vol. 2350, Videometrics III, pp. 306-321.

El-Hakim, S.F., Boulanger, P., Blais, F, Beraldin, J.-A., 1997. "A system for indoor 3D mapping and virtual environments, SPIE Proc., Vol. 3174, Videometrics V, pp. 21-35.

Feedema, J.T. & Little, C.Q., 1997. Rapid world modelling: Fitting Range Data to Geometric Prmitives. Proc. IEEE Int.Conf. on Robotics and Automation, Alberquerque, New Mexico, April 1997, pp 2807-2812.

Johnson, A.E., Hoffman, R., Osborn, J., Hebert, M., 1997. A System for semi-automatic modeling of complex environments, Proc. International Conference on Recent Advances in 3-D Digital Imaging and Modeling, Ottawa, pp. 213-220.

Miyatsuka, Y., Chen, X., Takahashi, Y., 1998. Archaeological 3D GIS for virtual museum in Damascus", Proc. ISPRS Comm. V, pp. 348- 355, Hakodate, Japan.

Rioux, M., 1984. Laser range finder based on synchronized scanners, *Applied Optic*s, **2**3, 3837-3844.

Roth, G., 1993. Extracting geometric primitives. CVGIP: ImageUnderstanding. Vol 58, No 1, July 1993, pp 1-22.